Partial Knowledge Distillation for Alleviating the Inherent Inter-Class Discrepancy in Federated Learning

Xiaoyu Gan, Xizi Chen, Jingyang Zhu, Xiaomeng Wang, Jingbo Jiang, and Chi-Ying Tsui

Abstract—Substantial efforts have been devoted to alleviating the impact of the long-tailed class distribution in federated learning. In this work, we observe an interesting phenomenon that weak classes consistently exist even for class-balanced learning. These weak classes, different from the minority classes in the previous works, are inherent to data and remain fairly consistent for various network structures and learning paradigms. The inherent inter-class accuracy discrepancy can reach over 36.9% for federated learning on the FashionMNIST and CIFAR-10 datasets, even when the class distribution is balanced both globally and locally. In this study, we empirically analyze the potential reason for this phenomenon. Furthermore, a partial knowledge distillation method is proposed to improve the model's classification accuracy for weak classes. In this approach, knowledge transfer is initiated upon the occurrence of specific misclassifications within certain weak classes. Experimental results show that the accuracy of weak classes can be improved by 10.7%, reducing the inherent inter-class discrepancy effectively.

Index Terms—Deep neural network, federated learning, class imbalance, weak class

I. INTRODUCTION

Federated learning (FL) is a decentralized machine learning paradigm where multiple clients collaborate to train a shared global model without directly sharing their local data [1]. This approach preserves data privacy by keeping the data on local devices. However, one big challenge to FL is the varying performance across different classes due to the presence of unbalanced sample sizes [2]. When the number of samples for different classes varies substantially, the global model often exhibits bias towards the majority classes, known as 'head classes'. The minority classes, referred as 'tail classes', become underrepresented [3], thus leading to lower classification accuracy as depicted in Fig. 1(a). However, in this work, we show that 'dominant' and 'weak' classes consistently exist even when sample sizes are equalized and samples from each class are uniformly distributed across the clients (i.e. with a balanced class distribution both globally and locally). Unlike the minority classes discussed in prior studies, these weak classes are inherent to the data itself, not dictated by sample size. The resulting inherent inter-class accuracy discrepancy (ICD) is illustrated in Fig. 1(b).

Fig. 2 presents the class-wise accuracy across several widely used benchmarks in the domain of FL. Each experiment is repeated five times, and the average result is presented. The ICD phenomenon identified in this study exhibits the following characteristics. 1) This phenomenon is universally present across different *learning paradigms* and especially pronounced in FL compared to centralized learning. 2) Models trained on the same dataset tend to exhibit a very similar ICD, indicating that this phenomenon is irrelevant to the *network structure*. 3) This phenomenon persists no matter whether the *local class distributions* in FL is balanced or not. Notably, as local imbalance intensifies, particularly when samples from weak classes are concentrated within a limited number of clients, the inherent ICD becomes significantly exacerbated. Details will be elaborated upon in the subsequent sections.

Although promising progress has been made in alleviating the inter-class discrepancy brought by class imbalance [3], these techniques cannot be directly applied to the inherent ICD problem.
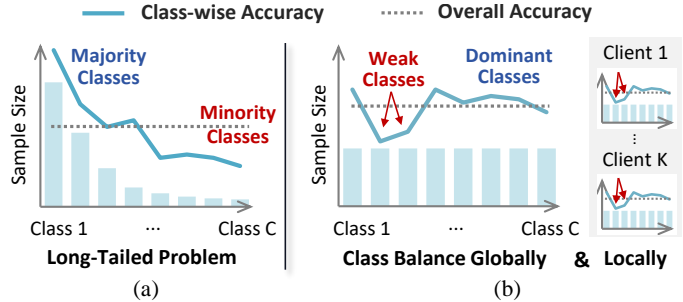

Fig. 1: (a) The Conventional Long-tailed Problem; (b) Inherent Inter-class Discrepancies Observed under Balanced Class Distributions (both Globally and Locally).

Specifically, current approaches usually focus on rebalancing class distributions by employing techniques such as over-sampling [4] or data augmentation [5] for the minority classes. However, considering that the inherent ICD is not associated with the quantity of samples, these methods may not be sufficient to mitigate the problem effectively.

Experiments indicate that a likely reason for this ICD phenomenon is the inherent similarity among the high-level feature representations of certain classes. This similarity poses a challenge for the classifier in accurately distinguishing data samples across these classes. In this work, we propose a federated partial knowledge distillation (PKD) method to improve classification accuracy for weak classes. Our method is inspired by the observation that an expert trained specifically on a group of confounding weak classes show greater proficiency in differentiating among them. This specialized model focuses solely on extracting and distinguishing the subtle feature differences among these classes and thus yields better accuracy than the model trained jointly on all classes. The term '**partial**' in PKD is shown in several aspects: 1) An expert's knowledge is confined to specific classes. It is tailored to identify a subset of data that shares analogous high-level features. 2) Knowledge distillation (KD) is triggered only when misclassifications between certain classes happens. Therefore, only a subset of the misclassified samples from these weak classes is considered in computing the KD loss during the training phase. 3) While there might be multiple experts, only up to one expert can be involved in the KD process for any given misclassified sample. Experimental results demonstrate that the proposed PKD method can effectively alleviate the inherent ICD issue by enhancing the classification accuracy of the worst performing classes. In summary, this work makes the following contributions:

- We highlight an interesting phenomenon that weak classes are always present, even in ideal scenarios where class distributions are balanced at both the global and local levels. This inherent variance in accuracy across different classes is especially pronounced in the context of FL, reaching up to 45.4% on the FashionMNIST dataset [6] and 36.9% on the CIFAR-10 dataset [7], respectively.
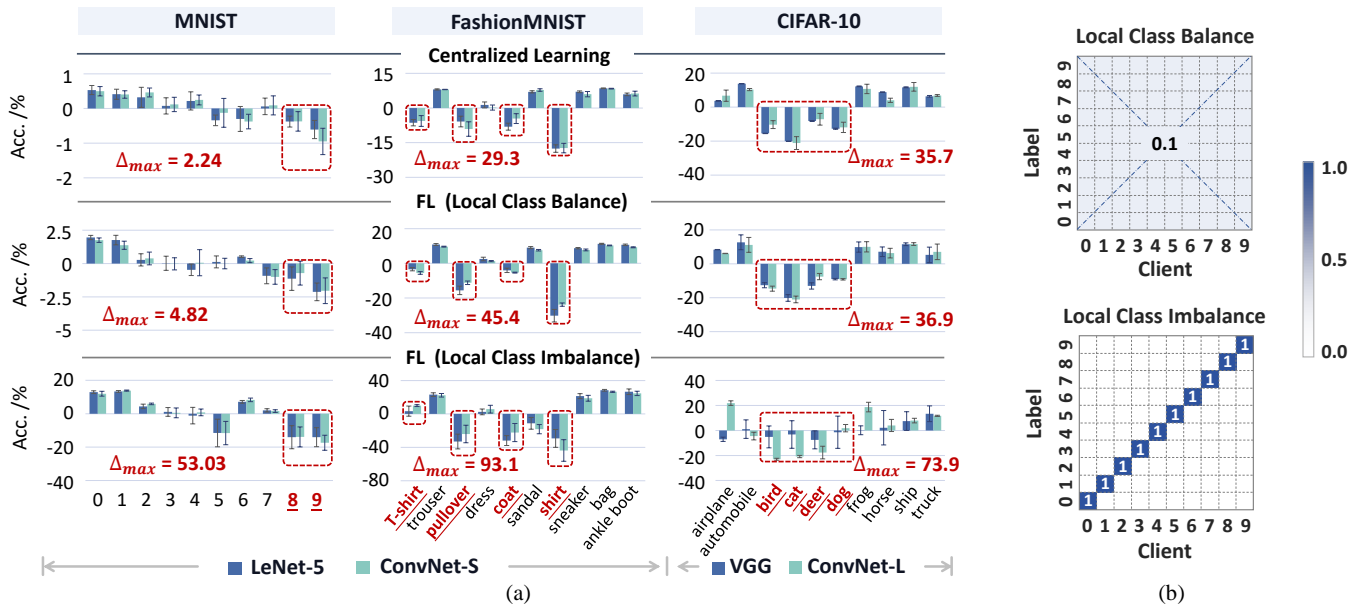
Fig. 2: (a) The Class-wise Accuracy (with Mean Subtraction) Based on Different Learning Paradigms and Network Structures (Δ: The Maximum Discrepancy in One Training); (b) Visualization of the Class Distribution Among 10 Clients.

- A federated partial KD method is proposed to enhance the learning process for weak classes. This approach selectively transfers knowledge from class-specific experts to the global student model, all within the FL framework.
- Experimental results show that the proposed method can effectively improve the classification accuracy of the weak classes by over 10.7% and 6.6% on FashionMNIST and CIFAR-10, respectively.

II. INTER-CLASS ACCURACY DISCREPANCY

A. Discrepancy Induced by the Class Imbalance Problem

ICD due to class imbalance. A primary reason for the variance in class-wise accuracy in deep learning is the imbalanced class distribution [8], [9]. The unbalanced sample sizes lead to a dual-fold challenge: 1) Models tend to be biased towards the majority classes, leaving the minority classes under-represented. 2) The lack of data for minority classes makes it even harder to learn the characteristics of these classes [3]. In federated learning, the potential causes for ICD become more complex. The presence of class imbalance at either the global level or within the local dataset of individual clients may diminish the model's quality. Besides, the mismatch in class distributions between the cloud and the clients may also degrade the performance of the global model [2]. Later we will show that the inherent ICD exits regardless of whether the local class distributions are balanced.

Existing approaches. Existing solutions can be broadly classified into several categories. 1) *Class re-balancing techniques*: These methods focus on offsetting the negative impact of uneven class distribution in training samples. This can be achieved by either over-sampling the minority classes to ensure a more equitable presence in the training data [4], [10], or by re-weighting the training loss values to mitigate the influence of uneven positive gradients [11], [12]. 2) *Data augmentation techniques*: These methods seek to enlarge the sample size or enhance the sample quality of minority classes through data augmentation techniques [13]–[15]. Compared to mere re-balancing methods, this approach can potentially enrich

the diversity within the minority classes, thereby reducing the risk of overfitting. 3) Other methods include meta-learning [16], ensemble learning [17], [18], transfer learning [17], and so on. Although significant progress has been achieved in reducing the ICD induced by class imbalance, such strategies may not be directly applicable to addressing the inherent ICD problem, as we will discuss below.

B. The Inherent ICD in This Work

Differences from the class imbalance problem. While the weak classes show similar poor accuracy to the minority classes in the class imbalance problem, their underlying causes and potential solutions are distinct. First, the inherent ICD is not a result of uneven sample sizes across different classes. Weak classes consistently exist even in the ideal case where both global and local data are class balanced. Consequently, previous methods that rely on re-sampling local data [14] or clients [19] based on their sample sizes are not feasible in this context. Second, in contrast to minority classes, weak classes are not characterized by data scarcity or a lack of diversity. Experimental results suggest that the conventional data augmentation techniques [20] fail to address the inherent ICD effectively, and in some cases, they might even intensify the inherent accuracy discrepancy.

The inherent ICD phenomenon. Fig. 2(a) shows the class-wise accuracy achieved on three datasets. In each scenario, the total number of samples for each class is kept identical, ensuring that global class balance is maintained. We adopt several commonly used convolutional neural networks and train the models following different learning paradigms. Two local data partition strategies are adopted in FL for each dataset, as illustrated in Fig. 2(b). Our results indicate that this inherent ICD is a common phenomenon across various network structures, learning paradigms, and local dataset partition strategies. Most of the dominant classes and the weak classes, e.g., {'0', '1'} and {'8', '9'} in MNIST [21], remain fairly consistent across various settings. The inter-class accuracy discrepancy is less marked for centralized learning and thus may go unnoticed. However, when it comes to FL, the discrepancy may increase significantly, e.g. reaching up to 45.4% for FashionMNIST. We also test the local class imbalance scenario using a pathological data partition strategy
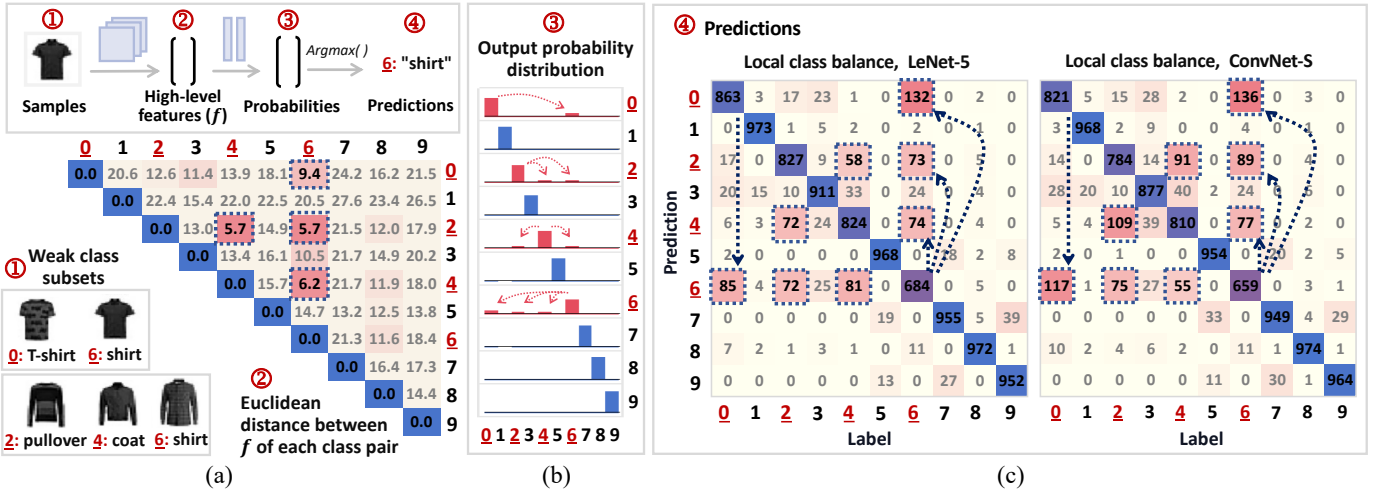
Fig. 3: FashionMNIST: (a) Raw Samples and the Similarity in High-Level Feature Representations between Each Pair of Classes; (b) Output Probabilities (Averaged over 1000 Samples per Class); (c) Prediction Results. For simplicity, each class is assigned a serial number. (0: T-shirt, 1: Trouser, 2: Pullover, 3: Dress, 4: Coat, 5: Sandal, 6: Shirt, 7: Sneaker, 8: Bag, 9: Ankle Boot.)
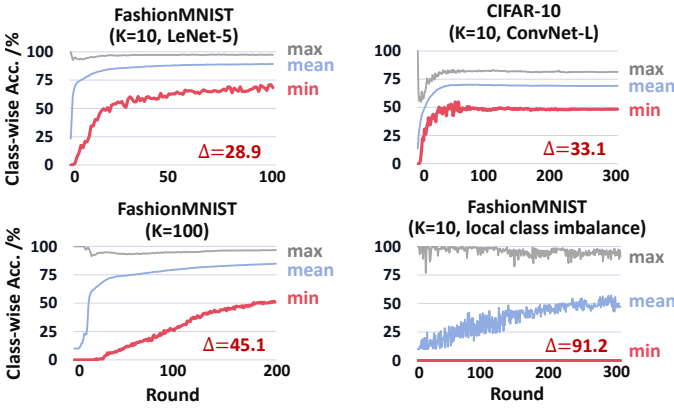

Fig. 4: The Maximum and Minimum Accuracy During Training. (K: Number of Clients Participating in FL at each Round)

proposed in [1]. Specifically, each client is assigned samples from a single class to ensure a clear and straightforward comparison of the class-wise accuracy. As shown in Fig. 2(a), the same group of weak classes is observed, with the accuracy discrepancy further increasing to a significant 53.0% on the MNIST dataset. For more complex datasets like FashionMNIST and CIFAR-10, such discrepancy can reach up to over 73.9%.

Fig. 4 shows the maximum and minimum class-wise accuracy at each round. While the overall accuracy rises smoothly over time, the difference between the maximum and minimum values continues to be evident. With a balanced class distribution globally and locally, the accuracy discrepancy on the FashionMNIST dataset is 28.9% when there are 10 clients selected at each round. This value increases significantly as the number of clients participating in FL grows to 100. In scenarios with local class imbalance, samples from weak classes are concentrated within a small subset of clients, thereby amplifying the accuracy discrepancy to 91.2%. The minimum class-wise accuracy is close to zero, indicating that the final model might completely fail in specific classes.

Potential reasons for inherent ICD. Fig. 3 (c) maps the predictions to the original classes to which the data belongs (the models are trained once). It shows that the negative samples of a weak class are often assigned certain wrong labels. For the FashionMNIST dataset with a balanced local class distribution, 62% ($=\frac{85}{137}$) of the misclassified 'T-shirt' samples are identified as 'shirts' using the LeNet-5 model [21]. Conversely, around 42% ($=\frac{132}{316}$) of the misclassified 'shirt' samples are labeled as 'T-shirts'. Another group of classes that can easily be confused with each other include {'pullover', 'coat', and 'shirt'}. For instance, 23% of the misclassified 'shirt' samples are identified as 'pullovers', while 23% are mistaken for 'coats'. That is to say, a total of 88% of the misclassified 'shirt' samples are incorrectly categorized as other weak classes. This phenomenon becomes particularly pronounced in scenarios with local class imbalance. Approximately 81% of the overall samples categorized under 'pullover' and 'coat' are misidentified as 'shirt' by the LeNet-5 model. A similar phenomenon is also observed with ConvNet, as shown in Fig. 3 (c).

Fig. 3(a) presents some misclassified samples from the two groups of weak classes, i.e. {'T-shirt', 'shirt'} and {'pullover', 'coat', 'shirt'}. It can be seen that these samples exhibit considerable similarities. Fig. 3(a) assesses the similarity in the high-level features between each pair of classes. The weak classes within the two aforementioned groups exhibit a lower Euclidean distance compared to the others, indicating a higher degree of similarity. As a result, it is challenging for the classifier to differentiate among these classes, leading to lower accuracy and reduced confidence in the model's predictions. The probability distributions determined by the softmax function are depicted in Fig. 3(b). The figure displays the average probability distribution across all samples within each class.

We further investigate how the classification accuracy for weak classes changes during training. As depicted in Fig. 5, the variance between two consecutive rounds can reach up to 80%, even when the global accuracy has become relatively stable. Furthermore, observations reveal a general trend within the group {'pullover', 'coat', 'shirt'}: an improvement in the accuracy of one class is accompanied by a corresponding decrease in another's. The collective accuracy across these three classes appears to be relatively stable. The value hovers around 1/3, implying that the model may be able to generally differentiate them from the dominant classes but fail to recognize the differences among them.
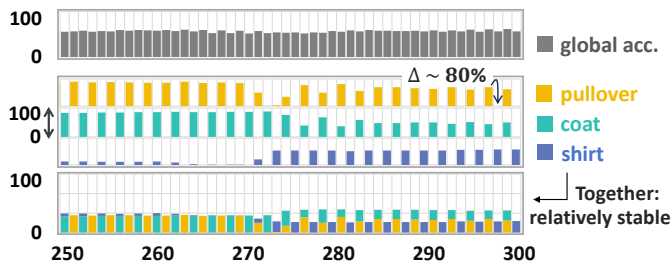
Fig. 5: The Class-wise Accuracy (%) During Training (FashionMNIST, Local Class Imbalance). X Axis: Rounds; Y Axis: Accuracy.

While FashionMNIST is used as an example for ease of illustration, similar phenomena are observed in other datasets as well. For instance, in the MNIST dataset, samples from the weak classes '8' and '9' are more likely to be misclassified as {'3', '5'} and {'4', '7'}, respectively. In the CIFAR-10 dataset, the four weak classes {'bird', 'cat', 'deer', 'dog'} are prone to confusion with one another. Interestingly, while these classes may not appear similar in their raw image forms, they exhibit similar high-level features that can make them challenging to distinguish for classification models.

III. THE PROPOSED ALGORITHM

A. Overview

In this work, we introduce a federated partial knowledge distillation (PKD) method to mitigate the impact of inherent ICD and enhance the classification accuracy of weak classes. The flow of the proposed method is outlined in Algorithm 1. The initial model first undergoes several rounds of federated learning (e.g. 10 to 20 rounds for FashionMNIST). After the warmup stage, it enters an expert learning phase. Weak classes are identified at the edge by examining the output probability distribution obtained from a feedforward pass on the local training set. Fig. 6 shows the predicted probabilities for classes other than the true class. Each curve represents the probability of samples from one class being misclassified as another class. As depicted in the figure, after the short warmup phase, the chance of misclassifying one weak class as another within the same group—such as a 'T-shirt' being predicted as a 'shirt' or vice versa—is significantly higher compared to other cases. This distinction can help to identify the weak class groups. The identified groups of weak classes demonstrate a notable consistency across different clients. g_i in Line 7 refers to a group of classes that can easily be confused with each other. For example, in FashionMNIST, g_1 consists of {'T-shirt', 'shirt'}, and g_2 comprises of {'pullover', 'coat', and 'shirt'}. In the case of CIFAR-10, there is only one group including {'bird', 'cat', 'deer' and 'dog'}. Once a group of weak classes is identified (g_i), a specialized expert model is trained on a subset of the training data (D_{g_i}) to extract and discern the subtle feature differences among them. All experts are trained within the FL framework, ensuring that no data is uploaded to the cloud. This process takes 25 local training rounds for the FashionMNIST dataset. Typically, one or two experts are adequate to address all the weak classes as described in Section II-B.

In the third stage, partial KD is implemented to transfer the class-specific knowledge from the specialized expert models to the student model, all within the FL framework. This approach is different from the conventional KD methods in several aspects. First, it is triggered only when misclassifications between certain classes (within g_i) happens, which means only a subset of misclassified samples is considered in computing the KD loss. Second, while there may be multiple experts, only one expert can be involved in the KD

Algorithm 1: Overview of the Proposed Method

Input: Number of Rounds (T_1, T_2, T_3); Training Set (D)
Output: Global Model (w)

1   Initialize w ;
2   **Stage 1: Warmup**
3   **for** $i \leftarrow 1$ **to** T_1 **do**
4 | $w \leftarrow$ FL(w, D) ;
5   **end**
6   **Stage 2: Expert Learning**
7   $g_1, g_2 \leftarrow$ identify-weak-class(w, D) ;
8   $exp_1, exp_2 \leftarrow$ create-expert(g_1, g_2) ;
9   **for** $i \leftarrow 1$ **to** T_2 **do**
10 | $exp_1 \leftarrow$ FL(D_{g_1}) ;
11 | $exp_2 \leftarrow$ FL(D_{g_2}) ;
12   **end**
13   **Stage 3: FL with KD**
14   **for** $i \leftarrow 1$ **to** T_3 **do**
15 | $w \leftarrow$ FL-with-PKD(w, exp_1, exp_2, D) ;
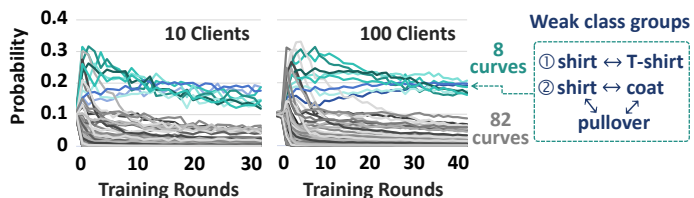16   **end**

Fig. 6: The Probability of Samples from One Class Being Misclassified as Another Class. (FashionMNIST: 90 Curves in Total)

process for any given misclassified sample. Further details regarding the partial KD process will be presented in the following subsection.

B. Partial Knowledge Distillation

The complete pseudo-code of the partial KD process is given in Algorithm 2. The overall framework is similar to the baseline approach of FedAvg [1], with the exception of the loss calculation described within the dashed box. At each round, the global model is broadcast to K randomly selected clients. Each client trains the model locally for E epochs using its own dataset (Line 5). Then, the local models are sent back and aggregated on the server (Line 7) as described in [1].

During the local training phase on client k, the prediction results are analyzed to detect any instances of misclassification among certain classes. An illustration example using the FashionMNIST dataset is presented in Fig. 7. Once misclassification within group g_i occurs, the corresponding expert model exp_i is triggered. A KD loss is then computed (Line 17 and 18) using the KL divergence [22] between p_s and p_e:

$$L_{KD} = D_{KL}(p_s \parallel p_e) \tag{1}$$

where p_s and p_e represent the predicted probabilities obtained from the student model and the expert model, respectively. The probabilities are calculated using the Softmax function with a temperature parameter T, formulated as follows:

$$p_i = \frac{e^{z_i/T}}{\sum_j e^{z_j/T}} \tag{2}$$

Algorithm 2: FL with Partial KD

Input: Experts (exp_1, exp_2); Global model (w);
# of rounds (T_3); # of clients each round (K);
# of local epochs (E); Batch size (B); Learning rate (η);
Training set (D)
Output: Global model (w)

1 —— **Server Executes** ——
2 **for** $t \leftarrow 1$ **to** T_3 **do**
3     $S_t \leftarrow$ random-select-clients(K) ;
4   **for** *each client* $k \in S_t$ *in parallel* **do**
5         $w_{t+1}^k \leftarrow$ client-update(k, w_t) ;
6   **end**
7     $w_{t+1} \leftarrow$ aggregate$(w_{t+1}^1, ..., w_{t+1}^K)$;
8 **end**
9 —— **Client Update** ——   // Run on client k
10 $\mathcal{B} \leftarrow$ split-into-batches(D_k, B) ;
11 **for** *each local epoch* $e \leftarrow 1$ **to** E **do**
12   **for** *batch* $\{x, labels\} \in \mathcal{B}$ **do**
13         $preds \leftarrow$ forward(w^k, x) ;
14         $exp_i \leftarrow$ activate-expert$(preds, labels)$;
15         $L_{KD} \leftarrow 0$;
16   **if** $exp_i != None$ **then**
17             $preds_i \leftarrow$ forward(exp_i, x) ;
18             $L_{KD} \leftarrow$ KL-loss$(preds, preds_i)$;
19   **end**
20         $L_{CE} \leftarrow$ CE-loss$(preds, labels)$;   `Partial`
21         $L \leftarrow L_{CE} + \lambda L_{KD}$;   `KD`
22         $w^k \leftarrow w^k - \eta \Delta L$;
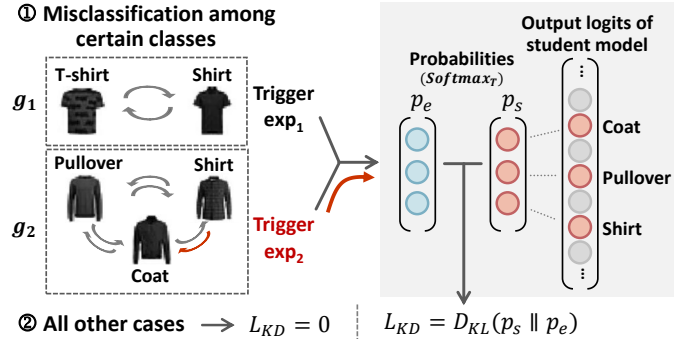23   **end**
24 **end**
25 **return** w^k to server ;

Fig. 7: An Illustration Example for the Partial KD Process.

activate the experts in round t. The value of $\sum_i n_{g_i}$ ranges from $0.4N$ to $0.6N$ for the three datasets. $\frac{n_{KD}^t}{E \cdot N}$ turns out to be a small value ranging from 0.003 to 0.16. Compared to the conventional KD methods, the overall computational overhead of the proposed partial KD method is significantly reduced. This reduction is attributed to the limited number of samples that participate in expert learning and the KD process. We will further demonstrate that with the same computational cost, the proposed method can achieve higher accuracy than the baseline FedAvg method.

IV. EXPERIMENTAL RESULTS

A. Experimental Setup

We evaluate the performance of our approach on three commonly used datasets in the field of FL: MNIST, FashionMNIST, and CIFAR-10. The data are partitioned in the same way as described in Section II-B. Two widely used neural networks, LeNet-5 and ConvNet-S as in [1], are deployed for the MNIST and FashionMNIST datasets, respectively. For the CIFAR-10 dataset, we employ larger networks including VGG-9 [23] and ConvNet-L (similar to ConvNet-S but with one more 5×5 Convolutional layer). In this section, we compare the performance of the PKD method with the baseline benchmark FedAvg, as well as several prior techniques designed to mitigate the ICD problem resulting from class imbalance. These techniques include focal loss [11] and data augmentation [14], [20]. Stochastic Gradient Descent is employed for optimization, with a learning rate set to 0.01. The number of local epochs and the batch size is optimized to 5 and 50, respectively. The models are trained for 100 rounds on MINIST and 300 rounds on the other datasets. The experts' network structure is identical to the global model's. The number of experts aligns with the weak class subsets detailed in Section II-B: two for MNIST and FashionMNIST, and one for CIFAR-10. During the PKD process, the hyperparameter T is set to 3. λ is tailored to 1 for both MNIST and FashionMNIST, and to 0.5 for CIFAR-10.

B. Performance of the Proposed Method

Table I presents the performance of our proposed method under conditions where the class distribution is balanced both globally and locally. In the baseline scenario, the inter-class accuracy discrepancy is 1.42%, 45.1% and 27.1% for MNIST, FashionMNIST and CIFAR-10, respectively. The proposed PKD method can improve the accuracy of the worst-performing classes by 0.4%, 10.7% and 6.6%, respectively, without comprising the global average accuracy. Furthermore, these improvements are more pronounced when the local class distribution is extremely unbalanced, as shown in Table I. In such cases, the minimum class-wise accuracy increases by 60.5% and 51.8% on MNIST and FashionMNIST, respectively. As shown

where z_i denotes the output logit. Since the partial KD method targets specific classes, p_s and p_e only involve a subset of classes, as illustrated in Fig. 7. In the case where no expert model is activated (exp_i = None in Line 16), L_{KD} is simply set to zero. The complete loss function is formulated as Line 21, where L_{CE} denotes the standard cross-entropy loss, and λ is a hyperparameter.

C. Overhead Analysis

While the proposed method can effectively improve the model's performance for weak classes, extra computational costs may be introduced by the expert training in stage 2 and the partial KD process in stage 3. Assuming the computational effort required for a local training round in the baseline scenario is denoted as U. The value can be calculated as follows:

$$U = E \cdot N \cdot (U_{FP} + U_{BP}) \tag{3}$$

where E and N denote the number of local epochs and the total number of samples across all C classes, respectively. U_{FP} and U_{BP} correspond to the computational loads for a forward pass and a backward pass, respectively. The number of computations per round for the proposed method is analyzed in detail as follows.

Stage 1: Warmup
$$U_{T_1} = U \tag{4}$$

Stage 2: Expert learning
$$U_{T_2} = E_{exp} \cdot \sum_i n_{g_i} \cdot (U_{FP} + U_{BP}) = \frac{E_{exp}}{E} \cdot \frac{\sum_i n_{g_i}}{N} \cdot U \tag{5}$$

Stage 3: FL with PKD
$$U_{T_3} = U + n_{KD}^t \cdot U_{FP} \approx (1 + \frac{1}{3} \cdot \frac{n_{KD}^t}{E \cdot N}) \cdot U \tag{6}$$

where n_{g_i} represents the number of samples belonging to the class group g_i, and n_{KD}^t denotes the number of misclassified samples that

TABLE I: Performance Evaluation of PKD in Comparison with FedAvg (With Global Class Balance in All Scenarios)

Dataset	MNIST						FashionMNIST												CIFAR-10		
Setup	Local Class Balance k=10			Local Class Imbalance k=10			Local Class Balance k=10			Local Class Balance k=100			Local Class Imbalance k=10			Local Class Balance k=10		
Method	FedAvg	PKD	Δ	FedAvg	PKD	Δ	FedAvg	PKD	Δ	FedAvg	PKD	Δ	FedAvg	PKD	Δ	FedAvg	PKD	Δ
Max.	99.73	99.73	**0.00**	96.02	99.03	**3.01**	97.30	97.60	**0.30**	96.70	96.60	**-0.10**	91.20	91.40	**0.20**	91.50	92.60	**1.10**
Ave.	99.28	99.32	**0.04**	75.85	84.45	**8.60**	89.29	89.50	**0.21**	84.66	84.72	**0.06**	47.39	71.03	**23.64**	82.80	83.25	**0.45**
Min.	98.31	98.71	**0.40**	7.90	68.38	**60.48**	68.40	76.60	**8.20**	51.60	62.30	**10.70**	0.00	51.80	**51.80**	64.40	71.00	**6.60**

TABLE II: Comparison of PKD with Other Methods

Dataset	FashionMNIST							
Setup	Local Class Balance, k=10							
Method	FedAvg [1]	Re-weighting [11]	Δ	Data Augmentation [20]	Δ	[14]	Δ	Ours PKD	Δ
Max.	97.30	97.80	**0.50**	97.40	**0.10**	97.40	**0.10**	97.60	**0.30**
Ave.	89.29	88.64	**-0.65**	85.04	**-4.25**	89.52	**0.23**	89.50	**0.21**
Min.	68.40	65.40	**-3.00**	53.80	**-14.6**	70.70	**2.30**	76.60	**8.20**

TABLE III: Computational Effort Required at Various Stages

Dataset	MNIST		FashionMNIST		CIFAR-10
Setup	Balance	Imbalance	Balance	Imbalance	Balance
U_{T_1}/U	1	1	1	1	1
U_{T_2}/U	0.6	0.6	0.5	0.08 (E=1)	0.4
U_{T_3}/U	1.0021	1.20	1.0274	1.13	1.0141

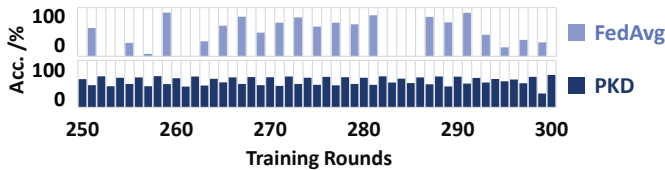* Balance: local class balance; Imbalance: local class imbalance.

Fig. 8: Accuracy of the Worst-Performing Class 'Shirt' During Training. (FashionMNIST, Local Class Imbalance as in Fig. 5)

in Fig. 8, the accuracy of weak classes becomes significantly more stable compared to the baseline case.

C. Comparison with Existing Techniques

Table II compares our proposed method with several existing techniques that address the ICD problem brought by class imbalance. An effective approach to address the class imbalance issue is to offset the negative impact brought by the uneven class distribution [11], [12]. It can be done by either re-sampling the minority classes or assigning larger weights to their loss values while calculating the empirical risk. Here we adopt a similar idea and test its performance for addressing the inherent ICD problem. Instead of up-weighting the minority classes, we dynamically enhance the weights of the inherent weak classes when calculating the loss value. The results indicate that the minimum class-wise accuracy may not be improved by this method. In [20] and [14], data augmentation is applied at the sample level and feature level, respectively, to implicitly enhance data diversity. These two approaches are commonly utilized to improve the model's performance on minority classes. The results suggest that feature-level data augmentation can modestly mitigate the inherent ICD issue, leading to a 2.30% improvement in the accuracy of the worst-performing class.

D. Overhead Analysis

Table III shows the computational effort required at various stages of the proposed method. The symbol U represents the computational load associated with a local training round in the baseline scenario. Since only a limited number of samples are involved in expert learning, the actual computational cost for stage 2 is less than $0.6U$. Since knowledge distillation is only applied under specific conditions, the computational overhead for stage 3 is less than $1.2U$. Fig. 9 (d) shows the frequency with which an expert is activated for KD. The value of $\frac{n_{KD}^t}{E \cdot N}$ in Eq. 6 increases rapidly at the onset of training
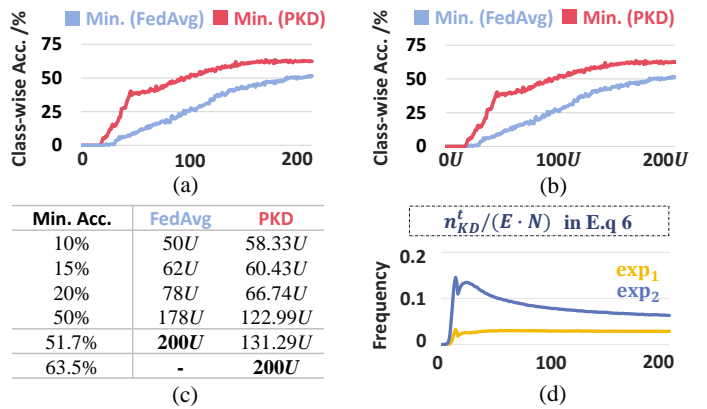

Fig. 9: (a) Accuracy at Different Training Rounds; (b) Accuracy with Different Amount of Local Computations; (c) Total Computations Required Across All Three Stages; (d) Expert Activating Frequency. (FashionMNIST, Global & Local Class Balance, 100 Clients)

and then gradually decreases as training progresses. KD occurs less frequently because, as the performance of the student model improves during training, fewer samples from the weak classes are misclassified.

Fig. 9(a) and (b) present the corresponding accuracy at different training rounds (PKD stage) and with varying amount of local computations. With an equivalent number of rounds, PKD incurs around 2.7% computation overhead in the local class balance scenario, as detailed in Table III. Nonetheless, since the model converges more rapidly than in the baseline scenario, fewer computations are necessary to achieve the same level of accuracy. For example, to achieve 50% accuracy for the worst-performing class, $178U$ computations are needed in the baseline scenario, whereas PKD requires only $123U$ computations. Before the PKD stage, the model has to undergo 20 rounds of warmup and 25 rounds of expert learning. The combined computational cost for these two phases is $32.5U$. Fig. 9(c) shows the accuracy levels versus the total amount of computations across all three stages.

V. CONCLUSION

In this work, we investigate an interesting phenomenon that weak classes consistently exist even for class-balanced learning. A class-specific partial knowledge distillation method is proposed to mitigate this inherent inter-class discrepancy.

REFERENCES

[1] B. McMahan, E. Moore, D. Ramage, S. Hampson, and B. A. y. Arcas, "Communication-Efficient Learning of Deep Networks from Decentralized Data," in *Proceedings of the 20th International Conference on Artificial Intelligence and Statistics*, ser. Proceedings of Machine Learning Research, A. Singh and J. Zhu, Eds., vol. 54. PMLR, 20–22 Apr 2017, pp. 1273–1282. [Online]. Available: https://proceedings.mlr.press/v54/mcmahan17a.html

[2] J. Zhang, C. Li, J. Qi, and J. He, "A survey on class imbalance in federated learning," 2023. [Online]. Available: https://arxiv.org/abs/2303.11673

[3] Y. Zhang, B. Kang, B. Hooi, S. Yan, and J. Feng, "Deep long-tailed learning: A survey," *IEEE Trans. Pattern Anal. Mach. Intell.*, vol. 45, no. 9, pp. 10 795–10 816, 2023.

[4] A. Estabrooks, T. Jo, and N. Japkowicz, "A multiple resampling method for learning from imbalanced data sets," *Comput. Intell.*, vol. 20, no. 1, pp. 18–36, 2004.

[5] J. Liu, Y. Sun, C. Han, Z. Dou, and W. Li, "Deep representation learning on long-tailed data: A learnable embedding augmentation perspective," in *2020 IEEE/CVF Conference on Computer Vision and Pattern Recognition, CVPR 2020, Seattle, WA, USA, June 13-19, 2020*. Computer Vision Foundation / IEEE, 2020, pp. 2967–2976.

[6] H. Xiao, K. Rasul, and R. Vollgraf, "Fashion-mnist: a novel image dataset for benchmarking machine learning algorithms," *CoRR*, vol. abs/1708.07747, 2017.

[7] A. Krizhevsky, "Learning multiple layers of features from tiny images," Univ. of Toronto, Toronto, Canada, Tech. Rep., 2009.

[8] H. He and E. A. Garcia, "Learning from imbalanced data," *IEEE Transactions on Knowledge and Data Engineering*, vol. 21, no. 9, pp. 1263–1284, 2009.

[9] M. Buda, A. Maki, and M. A. Mazurowski, "A systematic study of the class imbalance problem in convolutional neural networks," *Neural Networks*, vol. 106, pp. 249–259, 2018. [Online]. Available: https://www.sciencedirect.com/science/article/pii/S0893608018302107

[10] B. Liu, H. Li, H. Kang, G. Hua, and N. Vasconcelos, "Breadcrumbs: Adversarial class-balanced sampling for long-tailed recognition," in *Computer Vision – ECCV 2022*, S. Avidan, G. Brostow, M. Cissé, G. M. Farinella, and T. Hassner, Eds. Cham: Springer Nature Switzerland, 2022, pp. 637–653.

[11] T. Lin, P. Goyal, R. B. Girshick, K. He, and P. Dollár, "Focal loss for dense object detection," *IEEE Trans. Pattern Anal. Mach. Intell.*, vol. 42, no. 2, pp. 318–327, 2020.

[12] Y. Cui, M. Jia, T. Lin, Y. Song, and S. J. Belongie, "Class-balanced loss based on effective number of samples," in *IEEE Conference on Computer Vision and Pattern Recognition, CVPR 2019, Long Beach, CA, USA, June 16-20, 2019*. Computer Vision Foundation / IEEE, 2019, pp. 9268–9277.

[13] N. V. Chawla, K. W. Bowyer, L. O. Hall, and W. P. Kegelmeyer, "SMOTE: synthetic minority over-sampling technique," *J. Artif. Intell. Res.*, vol. 16, pp. 321–357, 2002. [Online]. Available: https://doi.org/10.1613/jair.953

[14] X. Shuai, Y. Shen, S. Jiang, Z. Zhao, Z. Yan, and G. Xing, "Balancefl: Addressing class imbalance in long-tail federated learning," in *21st ACM/IEEE International Conference on Information Processing in Sensor Networks, IPSN 2022, Milano, Italy, May 4-6, 2022*. IEEE, 2022, pp. 271–284. [Online]. Available: https://doi.org/10.1109/IPSN54338.2022.00029

[15] J. Kim, J. Jeong, and J. Shin, "M2m: Imbalanced classification via major-to-minor translation," in *2020 IEEE/CVF Conference on Computer Vision and Pattern Recognition, CVPR 2020, Seattle, WA, USA, June 13-19, 2020*. Computer Vision Foundation / IEEE, 2020, pp. 13 893–13 902.

[16] J. Ren, C. Yu, s. sheng, X. Ma, H. Zhao, S. Yi, and h. Li, "Balanced meta-softmax for long-tailed visual recognition," in *Advances in Neural Information Processing Systems*, H. Larochelle, M. Ranzato, R. Hadsell, M. Balcan, and H. Lin, Eds., vol. 33. Curran Associates, Inc., 2020, pp. 4175–4186.

[17] L. Xiang, G. Ding, and J. Han, "Learning from multiple experts: Self-paced knowledge distillation for long-tailed classification," in *Computer Vision - ECCV 2020 - 16th European Conference, Glasgow, UK, August 23-28, 2020, Proceedings, Part V*, ser. Lecture Notes in Computer Science, A. Vedaldi, H. Bischof, T. Brox, and J. Frahm, Eds., vol. 12350. Springer, 2020, pp. 247–263. [Online]. Available: https://doi.org/10.1007/978-3-030-58558-7_15

[18] J. Cui, S. Liu, Z. Tian, Z. Zhong, and J. Jia, "Reslt: Residual learning for long-tailed recognition," *IEEE Transactions on Pattern Analysis and Machine Intelligence*, vol. 45, no. 3, pp. 3695–3706, 2023.

[19] F. Zhao, Y. Huang, A. M. V. V. Sai, and Y. Wu, "A cluster-based solution to achieve fairness in federated learning," in *2020 IEEE Intl Conf on Parallel & Distributed Processing with Applications, Big Data & Cloud Computing, Sustainable Computing & Communications, Social Computing & Networking (ISPA/BDCloud/SocialCom/SustainCom)*, 2020, pp. 875–882.

[20] T. Devries and G. W. Taylor, "Improved regularization of convolutional neural networks with cutout," *CoRR*, vol. abs/1708.04552, 2017. [Online]. Available: http://arxiv.org/abs/1708.04552

[21] Y. Lecun, L. Bottou, Y. Bengio, and P. Haffner, "Gradient-based learning applied to document recognition," *Proceedings of the IEEE*, vol. 86, no. 11, pp. 2278–2324, 1998.

[22] G. Hinton, O. Vinyals, and J. Dean, "Distilling the knowledge in a neural network," 2015. [Online]. Available: https://arxiv.org/abs/1503.02531

[23] K. Simonyan and A. Zisserman, "Very deep convolutional networks for large-scale image recognition," *arXiv preprint arXiv:1409.1556*, 2014.